ACS APPLIED MATERIALS & INTERFACES

Research Article

www.acsami.org

Detection of ADAMTS-4 Activity Using a Fluorogenic Peptide-Conjugated Au Nanoparticle Probe in Human Knee Synovial Fluid

Shi Peng,[†,‡] Qiang Zheng,[‡,§] Xin Zhang,[†] Linghui Dai,[†] Jingxian Zhu,[†] Yanbin Pi,[†] Xiaoqing Hu,[†] Wenqing Cheng,[†] Chunyan Zhou,[⊥] Yinlin Sha,*[,§] and Yingfang Ao*[,†]

[†]Institute of Sports Medicine, Peking University Third Hospital, 49 North Garden Road, Haidian District, Beijing 100191, P. R. China

[§]Single-molecule and Nanobiology Laboratory, Department of Biophysics, School of Basic Medical Sciences, and Biomed-X Center, Peking University, 38 North Garden Road, Haidian District,Beijing 100191, P. R. China

[⊥]Department of Biochemistry and Molecular Biology, Peking University School of Basic Medical Sciences, 38 Xueyuan Road, Haidian District, Beijing 100191, P. R. China

Supporting Information

ABSTRACT: A disintegrin and metalloproteinase with thrombospondin motif-4 (ADAMTS-4) plays a pivotal role in degrading aggrecan, which is an early event in cartilage degrading joint diseases such as osteoarthritis (OA). Detection of ADAMTS-4 activity could provide useful clinical information for early diagnosis of such diseases and disease-modifying therapy. Therefore, we developed a ADAMTS-4 detective fluorescent turn-on AuNP probe (ADAMTS-4-D-Au probe) by conjugating gold nanoparticles with a FITC-modified ADAMTS-4-specific peptide (DVQEFRGVTAVIR). When the ADAMTS-4-D-Au probe was incubated with ADAMTS-4, the fluorescence recovered and fluorescence intensity markedly increased in proportion to concentrations of ADAMTS-4 and the probe. A nearly 3-fold increase in fluorescent intensity in response to only 3.9 pM of ADAMTS-4 was detected, whereas almost no fluorescence recovery was observed when the probe was incubated with matrix metalloproteinase (MMP)-1, -3, and -13. These results indicate a relative high sensitivity and specificity of the probe. Moreover, ADAMTS-4-D-Au probe was used to detect ADAMTS-4 activity in synovial fluid from 11 knee surgery patients. A substantial increase in fluorescent intensity was observed in the acute joint injury group as compared to the chronic joint injury and end-stage OA groups, indicating that this simple and low-cost sensing system might serve as a new detection method for ADAMTS-4 activity in biological samples and in screens for inhibitors for ADAMTS-4-related joint diseases. Additionally, this probe could be a potential biomarker for early diagnosis of cartilage-degrading joint diseases.

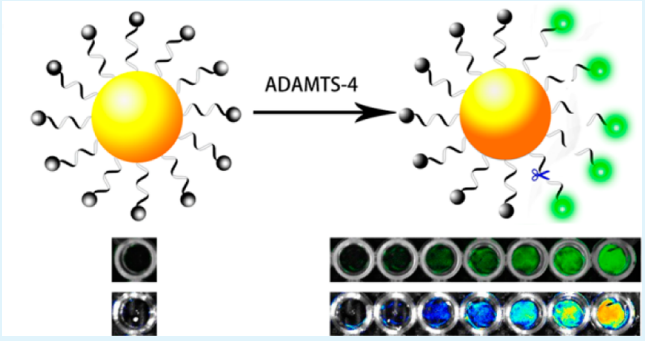

KEYWORDS: *ADAMTS-4, gold nanoparticles, osteoarthritis, fluorescent probe, synovial fluid*

INTRODUCTION

Gold nanoparticles (AuNPs)[1] are one of the most commonly used quenching materials in "turn-on" fluorescent sensing systems because of their distinct optical properties, such as high extinction coefficients[2] and localized surface plasmon resonance (LSPR).[3] Additionally, because of their chemical properties, the surfaces of AuNPs can be easily modified with various molecules (proteins, nucleic acids, silanols, and sugars) through strong covalent bonding or physical adsorption.[4,5] Therefore, AuNP-based turn-on fluorescent probes have been developed for the detection of ions,[6] small molecules,[7] and enzymes.[8]

A disintegrin and metalloproteinase with thrombospondin motif-4 (ADAMTS-4), which was first purified and cloned in 1999, is identified as an aggrecanase, as it can cleave aggrecan interglobular domain (IGD) at the Glu373-Ala374 bond.[9,10] Although aggrecanase plays a role in normal turnover of human cartilage aggrecan,[11,12] it is thought that elevation of activity in vitro is destructive to cartilage aggrecan.[13−15] Loss of aggrecan is considered to be a critical early event in the destruction of articular cartilage,[16] followed by degradation of collagen fibrils and irreversible mechanical failure of tissue.[17] Therefore, ADAMTS-4 could be an important biomarker for early diagnosis of cartilage destruction diseases such as OA.

ADAMTS-4 has gained much interest as a therapy target.[18] It has been demonstrated that direct blockage of ADAMTS-4/5 by an ADAM-TS inhibitor suppressed the loss of glycosaminoglycan (GAG) from OA cartilage, which could be potentially therapeutic in OA.[19] Other indirect therapies for OA, including glucosamine and chondroitin sulfate, may also partially inhibit the proinflammatory pathways that lead to downregulation of

Received: March 7, 2013
Accepted: May 28, 2013
Published: May 28, 2013

ADAMTS activity according to in vitro studies and animal models.[18] Therefore, detection of ADAMTS-4 activity might provide some insights not only into the initiation and progression of OA, but also into the effects of therapy.

ADAMTS-4 is synthesized as a preproprotein and activated by removal of a propeptide domain.[17] The existing methods to detect ADAMTS-4, including ELISA and Western blotting[20] rely on anti-ADAMTS-4 antibodies, are often used to determine the total amount of the enzyme, ixcluding the active and proenzyme form. Additional methods of studying ADAMTS-4 activity use antineoepitope antibodies[21,22] to the relative "large" substrates, which are either natural or recombinant forms of aggrecan, or peptides spanning the cleavage site of the aggrecan. Antineoepitope antibodies lack specificity for a specific enzyme, because some neo-peptides can also be produced by ADAMTS-5 and MMP.[20] Additionally, they are not suitable for high-throughput detection of ADAMTS enzyme activity and screening of potential inhibitors.[23] To date, there are only a few ways to directly detect the activity of ADAMTS-4. Recently, several short peptide substrate containing 13-mer peptides were screened using phage display.[24] These peptides were shown to be specific to ADAMTS-4, because they could not be cleaved by ADAMTS-5, which makes them suitable substrates for exploring the enzymatic activity and inhibitor development of ADAMTS-4.

In this study, we designed a ADAMTS-4 detective fluorescent turn-on AuNP probe (ADAMTS-4-D-Au probe) (Scheme 1) to detect ADAMTS-4 activity in human synovial fluid, such that it could serve as a new method to directly detect ADAMTS-4 activity in biological samples. An ADAMTS-4-specific 13-mer peptide, DVQEFRGVTAVIR (Asp-Val-Gln-Glu-Phe-Arg-Gly-Val-Thr-Ala-Val-Ile-Arg), used in this study was screened previously.[24] Fluorescein isothiocyanate (FITC), which can be quenched when it is close to AuNPs, was connected to the N-terminal of the peptide. The FITC-peptide was conjugated to Au nanoparticles 7 nm in diameter through a cysteine by gold−thiol bond, resulting in the ADAMTS-4-D-Au probe. Next, we explored the fluorescence generated by cleavage of the peptide by ADAMTS-4, thereby monitoring the enzymatic activity of ADAMTS-4. Finally, synovial fluids from patients undergoing knee surgery (total knee replacement and cruciate ligament or/and meniscal reconstruction surgeries) were measured for ADAMTS-4 activity.

Scheme 1. Illustration of ADAMTS-4 Detective Fluorescent Turn-on Peptide-Conjugated AuNP Probe (ADAMTS-4-D-Au probe) for the Detection of ADAMTS-4

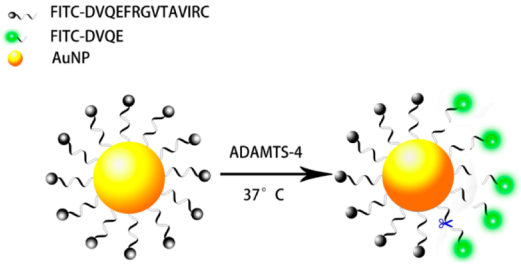

EXPERIMENTAL SECTION

Preparation of 7 nm Au Nanoparticles. AuNPs were produced by reduction of $HAuCl_4 \bullet 3H_2O$ (Aladdin Reagent Inc. Shanghai, China). Briefly, 0.5 mL of 1.0% $HAuCl_4$ was added to a reaction flask containing 47 mL of deionized water. The solution was heated to 60 °C followed by rapid addition of a mixture of 2 mL of 1% sodium bcitrate (Sigma-Aldrich) and 50 μL of 1.0% tannic acid (Sigma-Aldrich). Then, the solution was heated to reflux and the reaction was allowed to continue under uniform and vigorous stirring for 1 min. The color of the solution changed from light yellow to a red wine color. Next, the pH value of AuNPs solution was adjusted to 7.0 and stored at 4 °C.

Preparation of FITC-DVQEFRGVTAVIRC Conjugated AuNPs. For conjugation of the peptide to AuNPs, a slightly modified method established previously[25] was used. FITC-conjugated DVQEFRGVTAVIRC peptide (FITC-Asp-Val-Gln-Glu-Phe-Arg-Gly-Val-Thr-Ala-Val-Ile-Arg-Cys) was purchased from GL Biochem Ltd. (Shanghai, China). Briefly, 1.0 mL of the FITC-peptide solution (1.0 mg/mL in deionized water) was added dropwise to 10 mL of AuNP solution at room temperature under vigorous stirring and the reaction was then maintained for 24 h. Excess peptide was collected by centrifugation at 16000 rpm for further calculation. The resulting particles were further washed 3 times with deionized water and stored at 4 °C.

Characterization of FITC-DVQEFRGVTAVIRC-Au (ADAMTS-4-D-Au probe). Transmission electron microscopy (TEM) images were obtained in a FEI Tecnai T20 transmission electron microscope at 200 kV with a point-to-point resolution of 0.35 nm. The samples were prepared by pipetting one drop of the nanoparticle suspension onto the carbon-coated copper grid (5−50 nm in thickness) and allowed to settle for 20 s. The residual solution was wicked away using an absorbent tissue. The nanoparticle size analysis was conducted by using Image J 1.34s.

Atomic force microscopy (AFM) images were recorded in tapping mode in air by using a MultiMode IV caning probe microscopy (Veeco, USA) and silicon tips (spring constant 40 N m− 1, freq. 300 kHz, RTESP, Veeco). The acquired images were analyzed using Nanoscope III v.5.12 r2 (Veeco).

Dynamic light scattering (DLS) analyses were performed using ZetaPlus Potential Analyzer (Brookhaven, America). All samples were diluted to a AuNPs concentration of 100 pM.

Fluorescence Spectroscopy. Fluorescence experiments were conducted on a Hitachi F-4500 fluorescence spectrometer with a xenon lamp and a 152 P photomultiplier tube as the detector. Good spectra were obtained with the slits set at 2.5 nm and an integration time of 1 s. The samples were placed in quartz cuvettes (1-cm path length). To calculate the amounts of FITC-peptide conjugated to AuNPs, a fluorescence intensity standard curve was obtained with various concentrations (1.5, 2.6, 5.5, 11.0, and 22.0 μM) of FITC-peptide that served as the standard.

UV−vis absorption spectra were obtained using TU-1901 UV−vis spectrophotometer (Persee General Instrument Inc. Beijing, China), which scanned a range over 400−750 nm, with a collimated deuterium lamp source having a resolution of 1 nm.

Bright-field images and UV absorbance in PBS, reaction buffer, reaction buffer with human serum albumin (HAS, 5.0 mg HAS dissolved in 1.0 mL reaction buffer) (SIGMA), and reaction buffer with human synovial fluid (HSF, 100 μL HSF added into reaction buffer to a total volume of 1.0 mL) were obtained to test the stability of the ADAMTS-4-D-Au probe under various conditions.

Fluorescent imaging was performed using the Maestro II Imaging System (CRI, Inc. excitation: 435−480 nm, emission: 500 long-pass) with samples loaded in a 96-well plate. The Maestro II Optical System consists of an optical head that includes a liquid crystal tunable filter (LCTF, with a bandwidth of 10 nm and a scanning wavelength range of 500−950 nm) with a custom designed, spectrally optimized lens system that relays the image to a scientific-grade megapixel CCD. The tunable filter automatically steps in 10-nm increments from 500−550 nm while the camera captures images at each wavelength with a constant 500 ms exposure (total acquisition time was about 12 s)

Detection of ADAMTS-4 Activity Using ADAMTS-4-D-Au Probe. To determine the optimal probe concentration, various concentrations of ADAMTS-4 specific FITC-DVQEFRGVTAVIRC-Au (ADAMTS-4-D-Au probe) nanoparticle probes (7.5, 15, 30, 40, 60, 80, 120, 240 μM) were incubated with 62.5 pM of human recombinant ADAMTS-4 (Anaspec) in reaction buffer (50 mM Tris·HCl, 5 mM $CaCl_2 \cdot 2H_2O$, 150 mM NaCl, pH 7.5) in a total volume of 100 μL at 37 °C for 1 h, and both fluorescence data and images were recorded by

Fluorescence Spectroscopy and the Mestro II system as soon as the reaction was stopped. To test the specificity of our probe, 60 μM probe was incubated with 62.5 pM ADAMTS-4 and 1.5 μM activated MMP-13 (Anaspec), 1.5 μM activated MMP-1 (Peprotech), and 1.5 μM activated MMP-3 (Peprotech) in reaction buffer at 37 °C in a total volume of 500 μL. Fluorescence was monitored at different time intervals (10, 20, 30, 60, 90, 120, and 180 min). To study the sensitivity of the probe, we incubated various concentrations of ADAMTS-4 (3.9, 7.8, 15.6, 31.2, 62.5, 125, 250 pM) with 60 μM probe in reaction buffer in a total volume of 100 μL for 1 h at 37 °C; the reaction was then stopped and both fluorescent data and images was recorded. It should be noted that each 100 μL reaction system was diluted to 500 μL to facilitate fluorescence detection, and prior to use, ADAMTS-4 was incubated in 37 °C water bath for 15 min, and inactive MMP-1, -3, and -13 were activated by incubation with APMA (Genmed, Shanghai, China) for 1 h at 37 °C.

Human Synovial Fluid Samples. Prior to collection of joint fluid, informed consents were obtained from each patient according to approved recommendations of the ethical review committee of Peking University Third Hospital. Synovial fluid was aspirated from patients undergoing knee surgery (total knee replacement and cruciate ligament or/and meniscal reconstruction surgeries). Patients were divided into 3 groups according to their clinical diagnosis and sample collection time (time from first diagnosis or injury to synovial fluid aspiration): acute joint injury (AI) with sample collecting time of 1−9 months; chronic joint injury (CI) with sample collecting time of 1−10 years; end-stage OA with total knee replacement. All synovial fluid samples were harvested without lavage or any other diluent and were then aliquoted in 100 μL samples. All samples were stored at −80 °C prior to enzyme activity assays and were subject to only one freeze−thaw event. All procedures were approved by the ethical review committee of Peking University Third Hospital (number IRB00006761−2010085).

Screening of ADAMTS-4 Activity from Human Synovial Fluid. Diluted synovial fluid was incubated with 60 μM probe in a total volume of 100 μL for 1 h at 37 °C. Then, 100 μL was diluted into 500 μL for fluorescence testing. Three synovial fluid aliquots per patients were measured and data obtained were expressed as the mean ± standard deviation.

Enzyme-Linked Immunosorbent Assay (ELISA) of ADAMTS-4 in Synovial Fluid. The concentration of ADAMTS-4 in the diluted synovial fluid was determined using an ELISA kit (USCNLIFE company, Missouri city, USA) according to the manufacturer's instructions. Results were expressed as the mean ± standard deviation of triplicate samples.

Statistical Analysis. Results were expressed as the mean ± standard deviation of triplicate samples. Statistical analysis was performed using SPSS. One-way analysis of variance (ANOVA) was performed. SNK-q was used for comparing means of different groups. A value of $P < 0.05$ was considered statistically significant.

RESULTS AND DISCUSSION

Synthesize and Characterization of ADAMTS-4-D-Au Probe. To generate the ADAMTS-4-D-Au probe, we first synthesized AuNPs by a typical wet-chemistry method involving the chemical reduction of gold chloride using sodium citrate;[26] then FITC- DVQEFRGVTAVIRC with a ADAMTS-4 cleavage site between Glu and Phe was conjugated to AuNPs via the thiol group of cysteine. Once the peptide was successfully conjugated to AuNPs, almost no fluorescence signal was detected under UV-light compared with the strong fluorescence signal of the FITC-peptide monomer (Figure 2a). The linkage was further confirmed by atomic force microscopy (AFM) in tapping mode. As shown in panels a and b in Figure 1, the synthesized nanoparticles were nearly monodispersed. No aggregation was found before and after peptide conjugation, whereas the overall particle size was increased from 6.6 ± 0.3 nm to 9.7 ± 0.5 nm after peptide conjugation. This change could be

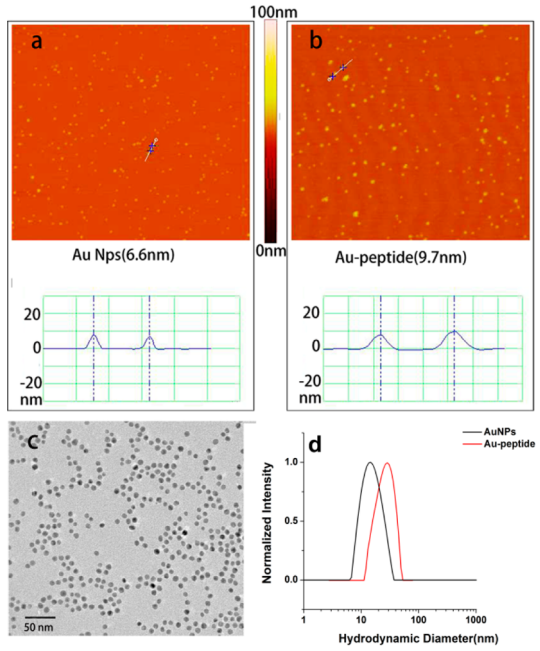

Figure 1. Morphological characterization of AuNPs and the ADAMTS-4-D-Au probe. (a) AFM image of the AuNPs. (b) AFM image of the ADAMTS-4-D-Au probe. (c) TEM image of the AuNPs. (d) Hydrodynamic diameter of AuNPs and ADAMTS-4-D-Au probe.

direct evidence of peptide linkage. More evidence was shown by DLS analyses, which showed that the hydrodynamic diameter had increased from 14.7 ± 4.3 nm to 29.6 ± 10.6 nm after peptide conjugation (Figure 1d). Transmission electron microscopy (TEM) analysis (Figure 1c) also showed that the probe was monodispersed. Due to the low electron density of the peptide layer, only the AuNPs core could be detected with the TEM technique, and the measured particle size was 7 nm (see Figure S3f in the Supporting Information), which was comparable to the size of unconjugated AuNPs measured by AFM.

To test the stability of the resulting ADAMTS-4-D-Au probe under various conditions, the ADAMTS-4-D-Au probe was dissolved in PBS, reaction buffer, reaction buffer with HSF, and reaction buffer with HSA, and multiple analytical methods (AFM, TEM, UV−vis Spectro, and DLS) were used to verify the results. As shown in Figure 2b, compared with the UV spectrum of bare AuNPs (LSPR peak at 520 nm), the ADAMTS-4-D-Au probe dissolved in PBS and reaction buffer showed only a ∼5 nm red-shift of the LSPR peak, which suggested that no aggregation of the ADAMTS-4-D-Au probe was formed in these solutions. The slight red-shift (<10 nm) might be caused by peptide conjugation. These conclusions were further supported by AFM (see Figure S2 in the Supporting Information), TEM (see Figure S3 in the Supporting Information), and DLS analyses (see Figure S4 in the Supporting Information). A more obvious red-shift was found in solutions of reaction buffer with HSF (∼10 nm), and reaction buffer with HAS (∼20 nm). Based on our AFM, TEM, and DLS analyses, we attributed this larger red-shift to the formation of some nanocomplexes in the presence of proteins. Additionally, the difference between these 2 samples might be explained by the much lower concentration of protein in synovial fluid than in buffer containing HAS.[27,28] Aggregation was infrequent in both samples, and most of the nanoparticles

dx.doi.org/10.1021/am400854z | ACS Appl. Mater. Interfaces 2013, 5, 6089−6096

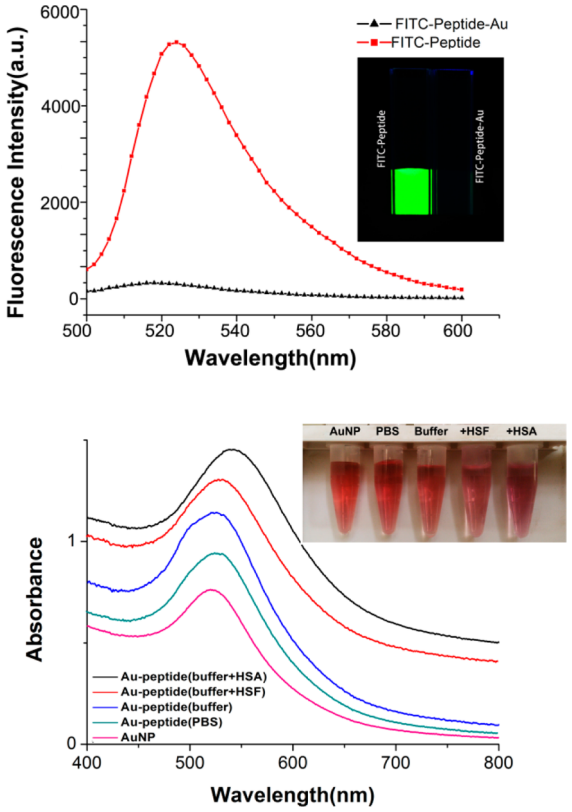

Figure 2. Spectral characterization of AuNPs and the ADAMTS-4-D-Au probe. (a) Fluorescence intensity of a FITC-peptide and the ADAMTS-4-D-Au probe. (b) UV absorbance and bright-field images of AuNPs and the ADAMTS-4-D-Au probe in various solutions (PBS, reaction buffer, reaction buffer + HSF, and reaction buffer + HSA) to test stability.

remained monodispersed over the course of the next 2 weeks. Collectively, these results suggested that the ADAMTS-4-D-Au probe was stable under various conditions and could be used to following catalytic reactions.

Detection of ADAMTS-4 Activity Using ADAMTS-4-D-Au Probe. The conjugated ADAMTS-4-D-Au probe showed almost no fluorescent signals in reaction buffer, because fo the quenching capacity of Au on the emitting fluorophores of FITC. When the probe was incubated with ADAMTS-4 in reaction buffer at 37 °C, fluorescence recovery signal was found to increase over time (Figure 3a). During the first 60 min, the enzymatic reaction proceeded at a relative high velocity, with a 12.5-fold fluorescence intensity increase at the 60-min point. After the first 60 min, the reaction velocity slowed down. At 180 min, an almost 14.5 fold increase of fluorescent intensity was observed. These results indicated that the ADAMTS-4-D-Au Probe was catalyzed by ADAMTS-4.

Next, we sought to determine the effectiveness of the ADAMTS-4-D-Au Probe by assessing optimal concentration, sensitivity, and specificity. To determine the probe concentration most suitable for ADAMTS-4 catalytic reactions, various concentration of ADAMTS-4-D-Au probe (7.5, 15, 30, 40, 60, 80, 120, 240 μM) were incubated with 62.5 pM ADAMTS-4. After a 1 h incubation, the fluorescence recovered was proportional to the concentration of the ADAMTS-4-D-Au probe (Figure 3b). Fluorescent signal was measured and a hyperbola curve was calculated according to ADAMTS-4-D-Au probe concentration (Figure 3b). The fluorescence signal was also

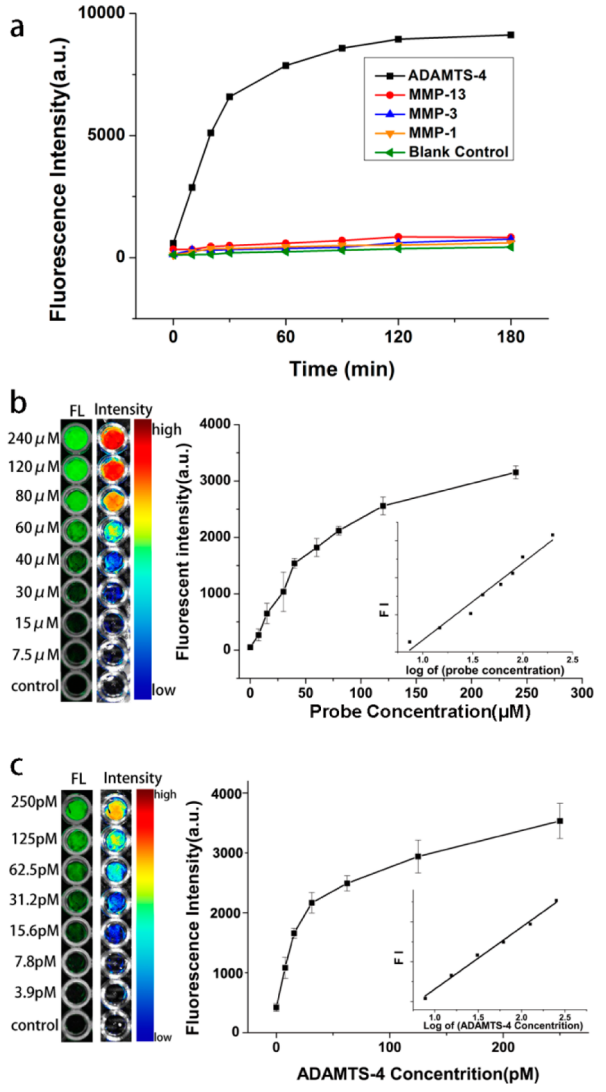

Figure 3. Detection of ADAMTS-4 activity using the ADAMTS-4-D-Au probe. (a) Fluorescence intensity curve of the ADAMTS-4-D-Au probe as a function of time in a 180 min time course at 37 °C after adding ADAMTS-4; activated MMP-1, MMP-3, and MMP-13; and reaction buffer as control. (b) Fluorescence images and intensity of various concentrations of the ADAMTS-4-D-Au probe in the presence of ADAMTS-4 for 1 h at 37 °C. (c) Fluorescence images and intensity of the ADAMTS-4-D-Au probe in the presence of various concentrations of ADAMTS-4 to test sensitivity.

replotted against the logarithm of the concentration of the ADAMTS-4-D-Au probe, and it showed a liner relationship (R^2 = 0.96, inset image in Figure 3b). To minimize the influence of the spectral quenching effect of AuNPs on released FITC and maintain detection sensitivity, we optimized the probe concentration to 60 μM and used it in subsequent experiments.

When various concentrations of ADAMTS-4 (3.9, 7.8, 15.6, 31.2, 62.5, 125, 250 pM) were added to the ADAMTS-4-D-Au probe, we observed a proportional relationship between ADAMTS-4 concentration and fluorescence recovery (Figure 3c). A hyperbola curve was drawn based on ADAMTS-4 concentration versus fluorescence intensity. A strong linear correlation (R^2 = 0.99) between fluorescence intensity and the logarithm of ADAMTS-4 concentration was confirmed (Figure 3c, inset). This indicated that we could establish a linear relation between fluorescence intensity and ADAMTS-4 concentration, thus allowing us to

dx.doi.org/10.1021/am400854z | ACS Appl. Mater. Interfaces 2013, 5, 6089−6096

calculate ADAMTS-4 activity directly using fluorescence signal. The theoretical detection limit (1.1 pM) was calculated based on a 3-fold standard deviation (SD) of the background and slope,which is comparable to the detection limit of ELISA (0.66pM). Importantly, in the experimental test we were able to detect a 3-fold increase of fluorescent signal in response to only 3.9 pM of ADAMTS-4 (Figure 3c), suggesting a high sensitivity of the probe. Because our goal was to use this probe to detect ADAMTS-4 activity in human synovial fluid, a biological sample containing protein, we repeated the above test in a reaction buffer containing human serum albumin (5 mg/mL) in order to correct the detection limit and linear range of quantification. As shown in Figure S5 in the Supporting Information, when the ADAMTS-4 concentration was in the range of 0 to 62.5 pM, both results were coincident: the hyperbola curves and the inset linear curves fit very well (see Figure S5 in the Supporting Information, dotted box). Additionally, the detection limit based on 3-fold standard deviation (SD) of background remained the same (1.1 pM). On the basis of our stability test results and the fact that the protein concentration in HSF is much lower than in human serum, we assume that the influence of protein content might be negligible when detecting ADAMTS-4 activity in HSF, and the linear range can be further extrapolated.

To test the specificity of the ADAMTS-4-D-Au probe, we used a reaction buffer as control and MMP-1, -3, and -13 with their activator were also used. During a 180 min time-course reaction, we observed almost no fluorescence recovery in the MMP-1, -3, and -13 groups and reaction buffer group (Figure 3a), while ADAMTS-4 exerted increasing fluorescence recovery intensity. These data suggested that the ADAMTS-4-D-Au Probe was specific for ADAMTS-4.

Relative high sensitivity and specificity of the ADAMTS-4-D-Au probe made it a suitable candidate for detection of ADATMS-4 activity. On the basis of the activity assay, our ADAMTS-4-D-Au probe was able to detect ADATMS-4 activity in a relatively simple and rapid method.

Screening of ADAMTS-4 Activity in Human Synovial Fluid. To monitor ADAMTS-4 activity in synovial fluid from patients undergoing knee surgery, we incubated 10 μL of synovial fluid with 60 μM ADAMTS-4-D-Au probe in reaction buffer in a total volume of 100 μL at 37 °C for 1 h. Altogether, 11 patients undergoing knee surgery were included in this study. The type of surgery is described in Table S1 in the Supporting Information.

Figure 4a showed that distinct fluorescence recovery was observed in all patients compared with blank control, suggesting that our ADAMTS-4-D-Au probe could be used to detect synovial fluid ADATMS-4 activity. Subsequently, all patients were divided into 3 groups according to clinical diagnosis and sample collecting time (see Table S1 in the Supporting Information): acute joint injury (AI), chronic joint injuries (CI), and total knee replacement due to end-stage osteoarthritis (OA). As shown in Figure 4c, AI patients presented the strongest fluorescent signals, 2.1-fold and 3.3-fold stronger than CI patients and end-stage OA patients, respectively. There were only small, nonsignificant difference between CI patients and end-stage OA patients.

Additionally, synovial fluid samples were analyzed by ELISA to detect the total amount of ADAMTS-4 (Figure 4a). As shown in figure 4b, ELISA results correlated well with fluorescence recovery in most samples (R^2 = 0.818, P = 0.002). However, two samples from the late-stage OA group showed a high

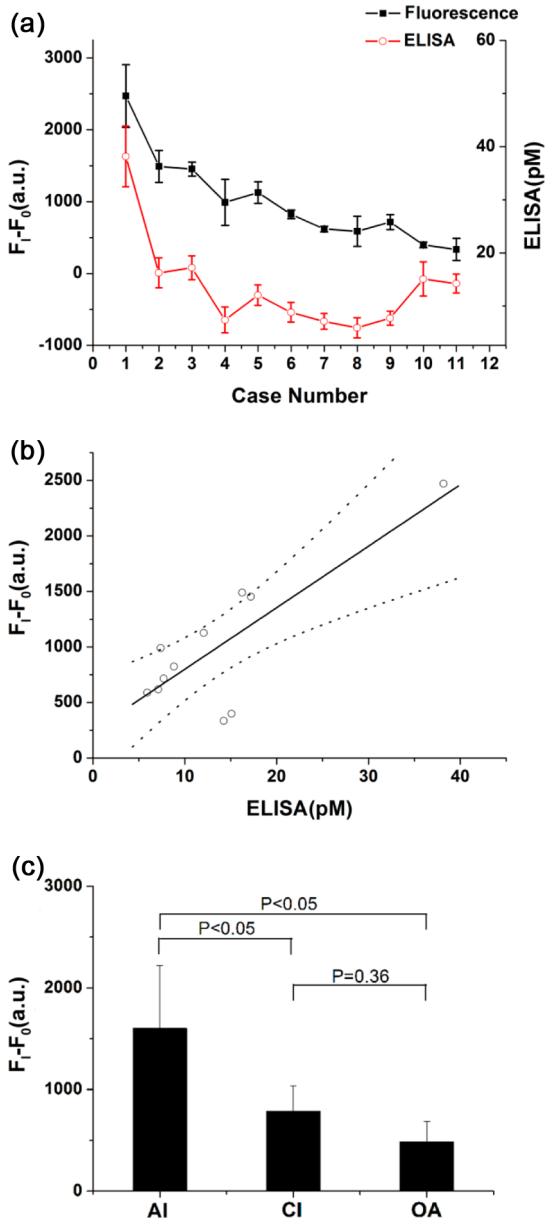

Figure 4. Application of the ADAMTS-4-D-Au probe in human synovial fluid. (a) Fluorescence intensity and ELISA of ADAMTS-4 in synovial fluid from 11 patients undergoing knee surgery. (b) Correlation between fluorescence intensity and ELISA in ADAMTS-4 quantification. Solid line shows the first order regression, and broken lines show the 95% confidence intervals. (F_1, measured fluorescence intensity, F_0, background fluorescence intensity). (c) Fluorescence intensity based on classification of the 11 patients, including acute joint injury (AI) (n = 4), chronic joint injury (CI) (n = 4), and end-stage OA with total knee replacement (OA) (n = 3).

concentration of ADAMTS-4 by ELISA, while the fluorescence recovery was weak. A possible explanation for this discrepancy might be the increasing release and expression of the inactive ADAMTS-4 proenzyme. ADAMTS-4 has been reported to be expressed in cartilage, joint capsule, synovial, and meniscus[29] and is synthesized as an inactive preproprotein intracellularly. Regulation of ADAMTS-4 at the protein level could be achieved by removal of the N-terminal pro-peptide domain or C-terminal spacer domain. In a late-stage OA joint, the cartilage is strongly damaged and synovitis is severe. These damaged

dx.doi.org/10.1021/am400854z | ACS Appl. Mater. Interfaces 2013, 5, 6089−6096

chondrocytes and synoviocytes may be released into the synovial fluid, resulting in increased release of inactive ADAMTS-4 from cells. Moreover, some studies have reported that mRNA expression of ADAMTS-4 increased in knee cartilage from patients with late-stage OA[30,31] and joint replacement surgeries,[14,19] which indicated that expression of the inactive proenzyme of ADAMTS-4 was increased in late-stage OA, while the activation was not increased accordingly.

Except for conventional ELISA using anti-ADAMTS-4 antibodies, other methods used to study aggrecanase activity, including sandwich ELISA[13] and Western blot[32] to quantify the amount of aggrecanase-generated ARGS fragments, have reported that ARGS fragments were elevated dramatically early after knee injuries. Our results, showing elevated ADAMTS-4 activity after acute knee injury, were consistent with these results. Additional studies, using electrochemiluminescence immunoassays to quantify aggrecanase-generated fragments[33,34] based on large sample sizes, have reported that increasing ARGS-fragments—on average 18 years after meniscectomy—are inversely associated with increased loss of joint space. This is likely due to a tissue repair response involving increased synthesis of aggrecan in combination with aggrecanase activity. One limitation of our current study is that we only included conventional ELISA as a comparison. We are, therefore, conducting studies with additional methods, used to detect aggrecanase-generated ARGS-fragments, on larger sample sizes to better explore aggrecanase activity, as an ongoing part of our project.

In 1 of our cases, when MRI and arthroscopy were employed, patient number 2 from the AI injury group showed arthroscopy with second degree cartilage damage (Figure 5c); on the other hand, the T_1-weighted and T_2-weighted MR images (Figure 5a, b) did not show signals relating to cartilage damage. However, high fluorescence intensity (Figure 4a) was observed in this patient, indicating that high ADAMTS-4 activity corresponded to the arthroscopy results. This indicated that the probe had the potential to be a biomarker for cartilage damage, which may not be detected by MRI.

Patients with acute joint injury or an anterior cruciate ligament tear accompanied with or without meniscus injuries are at high risk for subsequent OA,[35] which affects more young individuals.[35] However, at present, cartilage degradation is diagnosed by X-ray, MRI, and arthroscopy, which is used as the "golden standard". However, these methods can only detect irreversible morphological damage, which indicates that OA had advanced into a relatively late stage. Therefore, diagnosis of the early stage of cartilage degradation, before any morphological change, is quite important. Because ADAMTS-4 plays a key role in aggrecan degradation, which is an early event of cartilage damage, our probe detecting ADAMTS-4 activity could be a potential biomarker for early diagnosis of cartilage-degrading diseases.

Therefore, in this study, we confirmed the utility of a newly designed ADAMTS-4-D-Au probe to detect ADAMTS-4 activity in synovial fluid from cartilage-damaged patients. Further studies on a large sample size are needed to explore the relationship between ADAMTS-4 activity and cartilage-damage diseases, which we are currently conducting as an ongoing project.

CONCLUSION

In summary, we presented a new fluorescence turn-on ADAMTS-4-D-Au probe for detecting ADAMTS-4 activity by using a simple, inexpensive method. The ADAMTS-4-D-Au probe was stable in physiological conditions, and the recovery of its fluorescence intensity was proportional to the active ADAMTS-4 concentration. When the ADAMTS-4-D-Au probe was used to detect ADAMTS-4 activity in human synovial fluid, AI patients showed the strongest fluorescence recovery compared with CI and late-stage OA patients. This probe can be used to detect ADAMTS-4 in biological samples, and might serve as a new method for studying the mechanisms of ADAMTS-4 and in screens for inhibitors. Additionally, this probe could be a potential biomarker for early diagnosis of cartilage-damage diseases. Finally, considering the universality of this simple and cost-effective sensing system, many other biomolecules could be used to fabricate various sensing probes for the purpose of assisting clinical diagnosis and therapy.

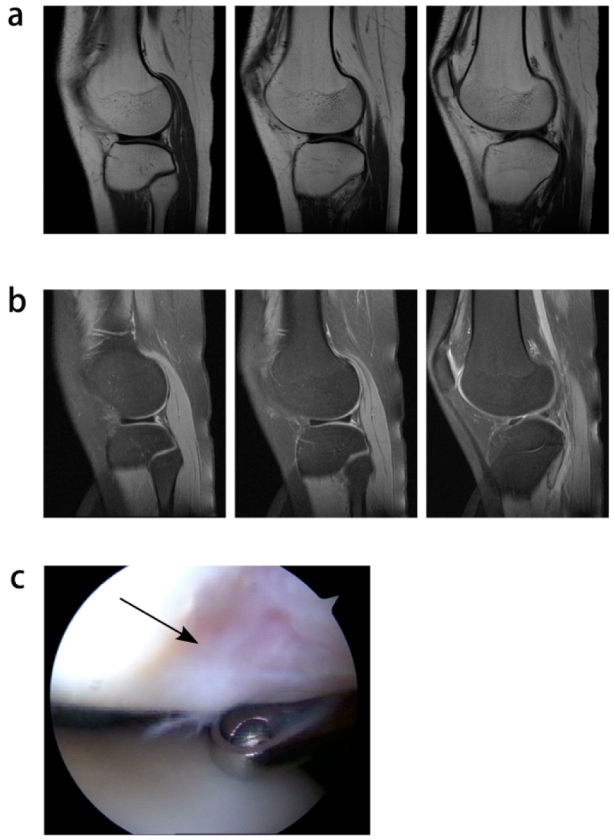

Figure 5. MR images and arthroscopic images of patient number 2. (a) T_1-weighted MR image of the external condyle of the femur shows no damage to cartilage. (b) T_2-weighted MR image of the external condyle of the femur shows no damage to cartilage. (c) Arthroscopic images of the external condyle of the femur shows second-degree cartilage damage (cartilage damage area was marked by black arrow).

ASSOCIATED CONTENT

Supporting Information

Table S1: Characteristics of the 11 patients providing synovial fluid samples. Figure S1: Calculation of the amount of FITC-peptide conjugated to Au nanoparticles. Figure S2: AFM images of AuNPs and AuNP-peptide in various solutions. Figure S3: TEM images of AuNPs and AuNP-peptide in various solutions. Figure S4: Hydrodynamic diameter of AuNPs and AuNP-peptide in various solutions. Figure S5: Fluorescence intensity of the ADAMTS-4-D-Au probe in reaction buffer and reaction buffer+HAS in the presence of various concentrations of ADAMTS-4. This material is available free of charge via the Internet at http://pubs.acs.org.

AUTHOR INFORMATION

Corresponding Author

*E-mail: yingfang.ao@vip.sina.com (Y.A.); shyl@hsc.pku.edu.cn (Y.S.).

Author Contributions

‡Authors S.P. and Q.Z. contributed equally to this work.

Author Contributions

The manuscript was written through contributions of all authors. All authors have given approval to the final version of the manuscript. S.P. and Q.Z. contributed to study conception and design, acquisition and interpretation of data, and drafting the manuscript. X.Z. and W.Q.C. contributed to collection of synovial fluid and related data interpretation. L.H.D. and Y.B.P. contributed to the statistical analysis and manuscript proofreading. L.H.D. and J.X.Z. contributed to the analysis of MRI and arthroscopic image. X.Q.H. contributed to the data interpretation of ELISA. C.Y.Z., Y.L.S., and Y.F.A. contributed to the conception and design, assisted with data analysis and interpretation, and helped to draft the manuscript. All authors have read and approved the final manuscript.

Notes

The authors declare no competing financial interest.

ACKNOWLEDGMENTS

This work was supported by grants from the Program of Sports Injury sponsored by the Ministry of Education of the People's Republic of China (Grant bmu2009129-112) and the National Natural Science Foundation of China (Grant 81071474).

ABBREVIATIONS

OA, osteoarthritis
GAG, glycosaminoglycan
FITC, Fluorescein isothiocyanate
PBS, phosphate-buffered saline
ADAMTS, a disintegrin and metalloproteinase with thrombospondin motifs
MMP, matrix metalloproteinases
SPR, surface plasmon resonance
IGD, aggrecan interglobular domain
CIA, collagen induced arthritis
AuNPs, gold nanoparticles
ADAMTS-4-D-Au probe, FITC-DVQEFRGVTAVIRC-Au
TEM, Transmission electron microscopy
AFM, Atomic Force Microscopy
AI, acute joint injury
CI, chronic joint injury
ELISA, Enzyme-linked immunosorbent assay
DI, deionized
APMA, 4-Aminophenylmercuric acetate
MRI, magnetic resonance imaging

REFERENCES

(1) Sardar, R.; Funston, A. M.; Mulvaney, P.; Murray, R. W. *Langmuir* **2009**, *25*, 13840−13851.
(2) Pissuwan, D.; Niidome, T.; Cortie, M. B. *J. Controlled Release* **2011**, *149*, 65−71.
(3) Murphy, C. J.; Gole, A. M.; Stone, J. W.; Sisco, P. N.; Alkilany, A. M.; Goldsmith, E. C.; Baxter, S. C. *Acc. Chem. Res.* **2008**, *41*, 1721−1730.
(4) Xu, X.; Daniel, W. L.; Wei, W.; Mirkin, C. A. *Small* **2010**, *6*, 623−626.
(5) Krpetic, Z.; Saleemi, S.; Prior, I. A.; See, V.; Qureshi, R.; Brust, M. *ACS Nano* **2011**, *5*, 5195−5201.
(6) Wei, S. C.; Hsu, P. H.; Lee, Y. F.; Lin, Y. W.; Huang, C. C. *ACS Appl. Mater. Interfaces* **2012**, *4*, 2652−2658.
(7) Radwan, S. H.; Azzazy, H. M. *Expert Rev. Mol. Diagn.* **2009**, *9*, 511−524.
(8) Gao, W.; Ji, L.; Li, L.; Cui, G.; Xu, K.; Li, P.; Tang, B. *Biomaterials* **2012**, *33*, 3710−3718.
(9) Abbaszade, I.; Liu, R. Q.; Yang, F.; Rosenfeld, S. A.; Ross, O. H.; Link, J. R.; Ellis, D. M.; Tortorella, M. D.; Pratta, M. A.; Hollis, J. M.; Wynn, R.; Duke, J. L.; George, H. J.; Hillman, M. C., Jr.; Murphy, K.; Wiswall, B. H.; Copeland, R. A.; Decicco, C. P.; Bruckner, R.; Nagase, H.; Itoh, Y.; Newton, R. C.; Magolda, R. L.; Trzaskos, J. M.; Hollis, G. F.; Arner, E. C.; Burn, T. C. *J. Biol. Chem.* **1999**, *274*, 23443−23450.
(10) Tortorella, M. D.; Burn, T. C.; Pratta, M. A.; Abbaszade, I.; Hollis, J. M.; Liu, R.; Rosenfeld, S. A.; Copeland, R. A.; Decicco, C. P.; Wynn, R.; Rockwell, A.; Yang, F.; Duke, J. L.; Solomon, K.; George, H.; Bruckner, R.; Nagase, H.; Itoh, Y.; Ellis, D. M.; Ross, H.; Wiswall, B. H.; Murphy, K.; Hillman, M. C., Jr.; Hollis, G. F.; Newton, R. C.; Magolda, R. L.; Trzaskos, J. M.; Arner, E. C. *Science* **1999**, *284*, 1664−1666.
(11) Bayliss, M. T.; Hutton, S.; Hayward, J.; Maciewicz, R. A. *Osteoarthritis Cartilage* **2001**, *9*, 553−560.
(12) Lark, M. W.; Bayne, E. K.; Flanagan, J.; Harper, C. F.; Hoerrner, L. A.; Hutchinson, N. I.; Singer, I. I.; Donatelli, S. A.; Weidner, J. R.; Williams, H. R.; Mumford, R. A.; Lohmander, L. S. *J. Clin. Invest.* **1997**, *100*, 93−106.
(13) Sandy, J. D.; Verscharen, C. *Biochem. J.* **2001**, *358*, 615−626.
(14) Naito, S.; Shiomi, T.; Okada, A.; Kimura, T.; Chijiiwa, M.; Fujita, Y.; Yatabe, T.; Komiya, K.; Enomoto, H.; Fujikawa, K.; Okada, Y. *Pathol. Int.* **2007**, *57*, 703−711.
(15) Song, R. H.; Tortorella, M. D.; Malfait, A. M.; Alston, J. T.; Yang, Z.; Arner, E. C.; Griggs, D. W. *Arthritis Rheum.* **2007**, *56*, 575−585.
(16) Mankin, H. J.; Lippiello, L. *J. Bone Joint Surg. Am.* **1970**, *52*, 424−434.
(17) Nagase, H.; Kashiwagi, M. *Arthritis Res. Ther.* **2003**, *5*, 94−103.
(18) Fosang, A. J.; Little, C. B. *Nat. Clin. Pract. Rheum.* **2008**, *4*, 420−427.
(19) Malfait, A. M.; Liu, R. Q.; Ijiri, K.; Komiya, S.; Tortorella, M. D. *J. Biol. Chem.* **2002**, *277*, 22201−22208.
(20) Tortorella, M. D.; Malfait, A. M.; Deccico, C.; Arner, E. *Osteoarthritis Cartilage* **2001**, *9*, 539−552.
(21) Tortorella, M. D.; Pratta, M.; Liu, R. Q.; Austin, J.; Ross, O. H.; Abbaszade, I.; Burn, T.; Arner, E. *J. Biol. Chem.* **2000**, *275*, 18566−18573.
(22) Pratta, M. A.; Su, J. L.; Leesnitzer, M. A.; Struglics, A.; Larsson, S.; Lohmander, L. S.; Kumar, S. *Osteoarthritis Cartilage* **2006**, *14*, 702−713.
(23) Miller, J. A.; Liu, R. Q.; Davis, G. L.; Pratta, M. A.; Trzaskos, J. M.; Copeland, R. A. *Anal. Biochem.* **2003**, *314*, 260−265.
(24) Hills, R.; Mazzarella, R.; Fok, K.; Liu, M.; Nemirovskiy, O.; Leone, J.; Zack, M. D.; Arner, E. C.; Viswanathan, M.; Abujoub, A.; Muruganandam, A.; Sexton, D. J.; Bassill, G. J.; Sato, A. K.; Malfait, A. M.; Tortorella, M. D. *J. Biol. Chem.* **2007**, *282*, 11101−11109.
(25) Kang, B.; Mackey, M. A.; El-Sayed, M. A. *J. Am. Chem. Soc.* **2010**, *132*, 1517−1519.
(26) Frens, G. *Nature Physical Science* **1973**, 20−22.
(27) Bani Ismail, Z.; Al-Rukibat, R. *J. Vet. Med., A* **2006**, *53*, 263−265.
(28) Chen, C. P.; Hsu, C. C.; Yeh, W. L.; Lin, H. C.; Hsieh, S. Y.; Lin, S. C.; Chen, T. T.; Chen, M. J.; Tang, S. F. *Proteome Sci.* **2011**, *9*, 65.
(29) Fosang, A. J.; Rogerson, F. M. *Osteoarthritis Cartilage* **2010**, *18*, 1109−1116.
(30) Bau, B.; Gebhard, P. M.; Haag, J.; Knorr, T.; Bartnik, E.; Aigner, T. *Arthritis Rheum.* **2002**, *46*, 2648−2657.
(31) Moulharat, N.; Lesur, C.; Thomas, M.; Rolland-Valognes, G.; Pastoureau, P.; Anract, P.; De Ceuninck, F.; Sabatini, M. *Osteoarthritis Cartilage* **2004**, *12*, 296−305.
(32) Larsson, S.; Lohmander, L. S.; Struglics, A. *Arthritis Res. Ther.* **2009**, *11*, R92.

(33) Larsson, S.; Englund, M.; Struglics, A.; Lohmander, L. S. *Arthritis Res. Ther.* **2010**, *12*, R230.
(34) Larsson, S.; Englund, M.; Struglics, A.; Lohmander, L. S. *Osteoarthritis Cartilage* **2012**, *20*, 388−395.
(35) Lotz, M. K.; Kraus, V. B. *Arthritis Res. Ther.* **2010**, *12*, 211.